AGU PUBLICATIONS

Geophysical Research Letters

RESEARCH LETTER
10.1002/2015GL064051

Key Points:
- We use a global ocean-atmosphere model to simulate atmospheric Hg trends
- Rapid warming and declining sea ice drive the unique Hg trends in the Arctic
- Suppressed deposition and enhanced evasion imply a decline of Arctic Ocean Hg

Correspondence to:
L. Chen and Y. Zhang,
chl@pku.edu.cn;
yxzhang@seas.harvard.edu

Citation:
Chen, L., Y. Zhang, D. J. Jacob, A. L. Soerensen, J. A. Fisher, H. M. Horowitz, E. S. Corbitt, and X. Wang (2015), A decline in Arctic Ocean mercury suggested by differences in decadal trends of atmospheric mercury between the Arctic and northern midlatitudes, *Geophys. Res. Lett.*, *42*, doi:10.1002/2015GL064051.

Received 31 MAR 2015
Accepted 28 MAY 2015
Accepted article online 1 JUN 2015

A decline in Arctic Ocean mercury suggested by differences in decadal trends of atmospheric mercury between the Arctic and northern midlatitudes

Long Chen[1,2], Yanxu Zhang[1], Daniel J. Jacob[1,3], Anne L. Soerensen[4,5], Jenny A. Fisher[6], Hannah M. Horowitz[3], Elizabeth S. Corbitt[3], and Xuejun Wang[2]

[1]School of Engineering and Applied Sciences, Harvard University, Cambridge, Massachusetts, USA, [2]Ministry of Education Laboratory of Earth Surface Processes, College of Urban and Environmental Sciences, Peking University, Beijing, China, [3]Department of Earth and Planetary Sciences, Harvard University, Cambridge, Massachusetts, USA, [4]Department of Environmental Science and Analytical Chemistry, Stockholm University, Stockholm, Sweden, [5]Department of Environmental Health, Harvard T. H. Chan School of Public Health, Boston, Massachusetts, USA, [6]School of Chemistry, University of Wollongong, Wollongong, New South Wales, Australia

Abstract Atmospheric mercury (Hg) in the Arctic shows much weaker or insignificant annual declines relative to northern midlatitudes over the past decade (2000–2009) but with strong seasonality in trends. We use a global ocean-atmosphere model of Hg (GEOS-Chem) to simulate these observed trends and determine the driving environmental variables. The atmospheric decline at northern midlatitudes can largely be explained by decreasing North Atlantic oceanic evasion. The midlatitude atmospheric signal propagates to the Arctic but is countered by rapid Arctic warming and declining sea ice, which suppresses deposition and promotes oceanic evasion over the Arctic Ocean. The resulting simulation implies a decline of Hg in the Arctic surface ocean that we estimate to be $-0.67\%\,yr^{-1}$ over the study period. Rapid Arctic warming and declining sea ice are projected for future decades and would drive a sustained decline in Arctic Ocean Hg, potentially alleviating the methylmercury exposure risk for northern populations.

1. Introduction

Anthropogenic releases of mercury (Hg) to the environment from coal combustion, mining, and use of Hg in commercial products and manufacturing processes have increased the global Hg loading in the surface ocean by an order of magnitude over natural levels [*Amos et al.*, 2013, 2014; *Horowitz et al.*, 2014]. Transport of Hg on a global scale takes place in the atmosphere via emission of elemental Hg^0, which has an atmospheric lifetime on the order of 0.5 years against oxidation to divalent Hg^{II} and subsequent deposition [*Lindberg et al.*, 2007; *Corbitt et al.*, 2011]. After deposition to the ocean, Hg can be methylated to toxic methylmercury which bioaccumulates and biomagnifies in marine food webs [*Mergler et al.*, 2007]. Hg pollution is of particular concern in the Arctic where populations rely heavily on marine-based diets [*Arctic Monitoring and Assessment Programme* (*AMAP*), 2011]. Here we examine trends in Arctic atmospheric Hg over the past decade (2000–2009) to better understand the factors controlling the sources of Hg in this part of the world.

Significant declines of atmospheric Hg have been observed at northern midlatitude regions over the past decade, including a decline of $-2.5\%\,yr^{-1}$ over the North Atlantic during 1990–2009 [*Soerensen et al.*, 2012]; -1.6 to $-2.0\%\,yr^{-1}$ at Mace Head, Ireland, during 1996–2009 [*Ebinghaus et al.*, 2011]; and an average decline of $-2.0\%\,yr^{-1}$ at four eastern Canadian sites during 2000–2009 [*Cole et al.*, 2013]. The decreasing North Atlantic oceanic evasion was speculated to compensate for the strongly increasing [*Streets et al.*, 2011] or relatively constant [*Wilson et al.*, 2010] anthropogenic emissions and subsequently explain these observed declining trends [*Soerensen et al.*, 2012]. Arctic atmospheric Hg shows a weaker decrease, and trends are more seasonally variable than at northern midlatitudes. For instance, weak annual declines ($-0.6\%\,yr^{-1}$ during 1995–2007; $-0.9\%\,yr^{-1}$ during 2000–2009) with significant increases in May and July were observed at Alert, Canada [*Cole and Steffen*, 2010; *Cole et al.*, 2013]. Atmospheric Hg at Zeppelin, Svalbard Island, was reported to have no overall annual trend but significantly increased in May, August, September, and October during 2000–2009 [*Berg et al.*, 2013].

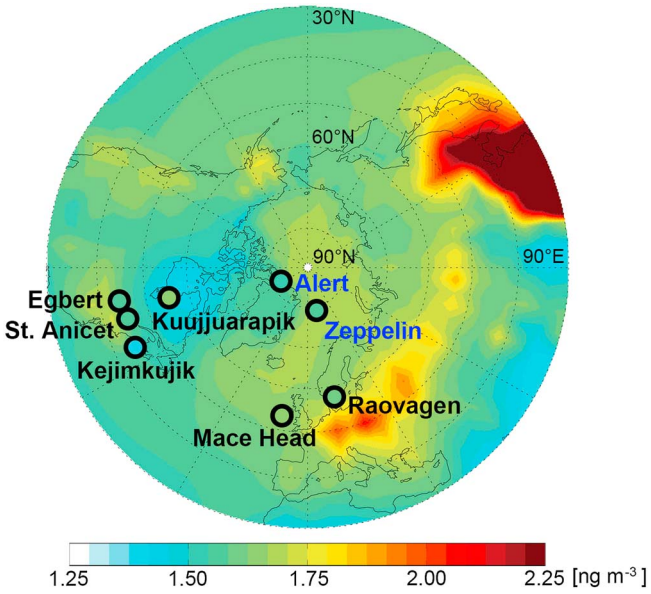

Figure 1. Mean total gaseous mercury (TGM) concentrations in 2000–2009 observed at long-term measurement sites (circles) (Arctic sites in blue and others in black) and simulated by the GEOS-Chem model in surface air (background).

The weaker and more seasonally variable trends suggest that Arctic atmospheric Hg is influenced not only by long-range transport from northern midlatitudes but also by its fast changing climate in recent decades [*Cole et al.*, 2013]. Surface air temperature in the Arctic has increased at a rate nearly 2 times faster than the global average [*Bekryaev et al.*, 2010], which could decrease the frequency and intensity of atmospheric mercury depletion events (AMDEs) in springtime and the subsequent deposition to the ocean [*Pöhler et al.*, 2010]. Sea ice extent over the Arctic Ocean has decreased by approximately 5–10% per decade [*Parkinson and Cavalieri*, 2008]. This increases the evasion of Hg^0 from the surface ocean, which is supersaturated relative to the atmosphere [*Andersson et al.*, 2008]. The increasing mobilization of Hg from thawing permafrost in the pan-Arctic regions [*Rydberg et al.*, 2010] along with the increasing freshwater discharge [*Shiklomanov and Lammers*, 2009] increases riverine Hg into the ocean [*Fisher et al.*, 2012].

Hypotheses have been proposed to explain the Arctic atmospheric Hg trends and interannual variability [*Cole et al.*, 2013; *Fisher et al.*, 2013], but how and what environmental variables drive the Hg trends and bring about the differences between the Arctic and northern midlatitudes are still not understood. Here we use a global ocean-atmosphere model of Hg (Goddard Earth Observing System Chemistry (GEOS-Chem)) to simulate the observed trends and determine the driving environmental variables.

2. Data and Model

2.1. Observational Sites

We use six northern midlatitude terrestrial sites and two Arctic sites (Alert and Zeppelin) with available observations during the last decade (2000–2009) from Canadian and European atmospheric mercury measurement networks (Canadian Atmospheric Mercury Measurement Network (CAMNet), 2014, http://www.ec.gc.ca/natchem/; European Monitoring and Evaluation Programme (EMEP), 2014, http://www.nilu.no/projects/ccc/) for trend analysis (Figure 1). Although the time series at Alert is longer (1995–2009), we use the data during 2000–2009 to keep consistency among sites. Taking the study period into account, we have limitation on location of Arctic sites.

Total gaseous mercury (TGM) (defined as the sum of Hg^0 and gaseous phase Hg^{II}) or Hg^0 is measured at these sites. However, they are not distinguished here because Hg^0 makes up approximately 95–99% of TGM in remote air [*Gustin and Jaffe*, 2010]. Daily values are used for calculation of observed monthly trends with nonparametric Mann-Kendall test and Sen's nonparametric estimator of slope [*Gilbert*, 1987]. Monthly values generated from the model are used to calculate simulated monthly trends with least squares linear regression. The frequencies of AMDEs over the Arctic sites are calculated as the fraction of hours with TGM concentrations below 1.0 ng m^{-3} [*Cobbett et al.*, 2007].

2.2. Model Description

We use the GEOS-Chem Hg model v9-01-02 (http://geos-chem.org) to simulate the atmospheric Hg trends in the Arctic and northern midlatitudes over the period 2000–2009. The GEOS-Chem Hg model includes a 3-D atmosphere model coupled to a 2-D surface slab ocean and a 2-D soil reservoir [*Holmes et al.*, 2010; *Soerensen*

Table 1. Selected Climatological Variables and Their Decadal Trends Over the Period 2000–2009[a]

Variables[b]	Unit	Decadal Trends of Variables (% yr^{-1})			
		November–March	April–May	June–July	August–October
Surface air temperature	K	*+0.06*[c]	+0.08	+0.02	+0.06
Sea surface temperature	K	+0.24	+0.10	*−0.02*	+0.06
Sea ice fraction	—	*+0.06*	*0*	*−0.08*	−2.49
Sea ice lead occurrence	h	+0.85	+0.84	*+0.84*	*−0.66*
Planetary boundary layer (PBL) depth	m	−0.76	−1.29	*−0.92*	*+0.30*
Net shortwave radiation	$W\,m^{-2}$	*+0.14*	+0.49	*−0.46*	*+0.12*
Surface wind speed	$m\,s^{-1}$	−0.37	*−0i26*	−0.72	+0.38
Freshwater discharge	$m^3\,s^{-1}$	—	*−1.78*	*+0.27*	+2.23
Net primary productivity (NPP)	$Tg\,C\,a^{-1}$	+2.18[d]			

[a]Trends are calculated based on the average data over the Arctic Ocean.
[b]Variables which are chosen for sensitivity simulations are derived from *Fisher et al.* [2013], and more details are shown in that study. Sea ice lead occurrence is used as proxy for sea ice threshold occurrence from *Fisher et al.* [2013]. Climatological variables are from the MERRA assimilated data [*Rienecker et al.*, 2011]. Freshwater discharge and net primary productivity are from the Arctic-Rapid Integrated Monitoring System (2014, http://rims.unh.edu/) and the NPP-sea ice extent relationship in *Arrigo and van Dijken* [2011], respectively.
[c]"+" indicates increasing trends and "−" indicates declining trends. Significant trends are indicated in normal fonts ($p \leq 0.1$), while insignificant trends are indicated in italics.
[d]Only annual data are available for NPP.

et al., 2010]. The model has 4° × 5° horizontal resolution and 47 vertical levels from the surface to 0.01 hPa. The model is driven by NASA Modern-Era Retrospective Analysis for Research and Applications (MERRA) assimilated meteorological data [*Rienecker et al.*, 2011]. The model tracks two Hg species in the atmosphere, Hg^0 and Hg^{II}, with oxidation of Hg^0 by Br atoms and photoreduction of Hg^{II} in cloud droplets [*Holmes et al.*, 2010]. High Br atom concentrations cause fast oxidation of Hg^0 to Hg^{II} and subsequent loss by deposition (i.e., AMDEs) in polar springtime [*Fisher et al.*, 2012].

The 2-D ocean mixed layer receives atmospheric Hg^{II} deposition and interacts with the atmosphere by air-sea exchange of Hg^0. There is also exchange with the subsurface ocean through particle settling and vertical transport [*Soerensen et al.*, 2010]. We specify the North Atlantic subsurface seawater Hg concentrations by yearly decreasing values from *Soerensen et al.* [2012] with imposed seasonal variability [*Mason et al.*, 2001; *Laurier et al.*, 2004]. Fixed concentrations are specified for other ocean basins [*Soerensen et al.*, 2010]. The model includes an ice/snow module as described by *Fisher et al.* [2012] and considers the interannual variability of riverine Hg [*Fisher et al.*, 2013].

The model is driven by Arctic Monitoring and Assessment Programme/United Nations Environment Programme anthropogenic emission inventories for the years 2000, 2005, and 2010 with linear interpolation for individual years. Global emissions slightly increased over the past decade (1819, 1921, and 1960 Mg for 2000, 2005, and 2010, respectively), with increase in Asia and decrease in North America and Europe [*Wilson et al.*, 2010; *AMAP/United Nations Environment Programme*, 2013].

2.3. Sensitivity Simulations

We determine the driving factors for the Arctic atmospheric Hg trends by evaluating a range of variables, including surface air temperature, sea surface temperature, sea ice fraction, sea ice lead occurrence, planetary boundary layer (PBL) depth, net shortwave radiation, surface wind speed, freshwater discharge, and net primary productivity (Table 1). For each variable, we run a sensitivity simulation in which the decadal trend of this variable is removed by repeating the data in the year 2000 for the entire simulation (2000–2009) over the Arctic region (68°N–90°N). We calculate the contribution of each variable by comparing with a base simulation without the trend removal.

3. Results and Discussion

3.1. Differences in Decadal Trends Between the Arctic and Northern Midlatitudes

Differences in atmospheric Hg trends between the Arctic and northern midlatitudes are illustrated in Figure 2. The observed monthly trends are consistently negative at midlatitude sites (six-site mean: $-0.030\,ng\,m^{-3}\,yr^{-1}$),

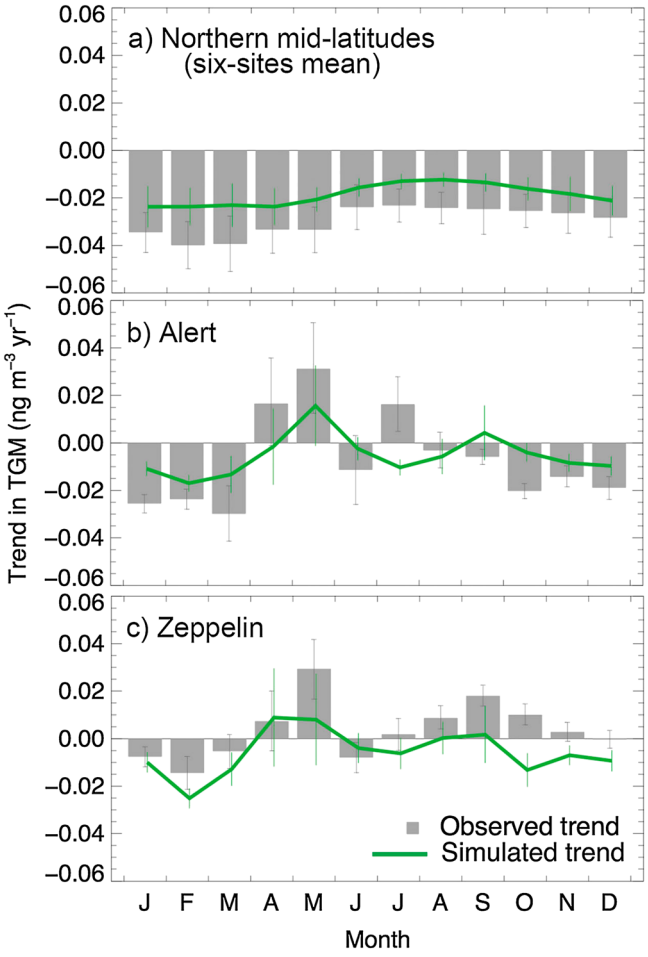

Figure 2. Monthly trends in total gaseous mercury (TGM) concentrations at (a) northern midlatitude sites (six-site mean) and (b and c) two Arctic sites over the period 2000–2009. The simulated values are sampled at the grid box containing the location of the site (accounting for latitude, longitude, and elevation). Standard deviations of the trends are shown as vertical bars.

and the seasonal variability is small (standard deviation: 0.006 ng m^{-3} yr^{-1}). The model predicts the monthly variability well ($R^2 = 0.79$; $p < 0.05$). Similar to *Soerensen et al.* [2012], the model simulation suggests that the declining trends at northern midlatitudes can be largely explained by the decreasing evasion that is caused by the declining subsurface seawater Hg concentrations in the North Atlantic. The decreasing anthropogenic emissions in North America and Europe may not be the cause as it is insufficient to compensate for the rise of emissions in Asia. The trends at midlatitude sites show a late winter maximum and a summer minimum in both observations and the model, mainly caused by the faster decreasing evasion rates from the North Atlantic in wintertime, when the surface ocean is more influenced by the subsurface ocean due to elevated entrainment and Ekman pumping [*Soerensen et al.*, 2010].

The observed annual trends at Alert and Zeppelin are -0.007 ± 0.019 and 0.003 ± 0.012 ng m^{-3} yr^{-1}, respectively, which are not significantly different from zero (i.e., no annual trends) but significantly smaller than at midlatitude sites ($p < 0.05$). Significant increases are observed in May and July at Alert and May, August, September, and October at Zeppelin, consistent with *Cole et al.* [2013], which suggests more variable monthly trends. The model captures the magnitudes of the observed trends as well as most of their seasonal variability at these sites, especially the increasing trends in spring and fall ($R^2 = 0.52$; $p < 0.05$).

The model fails to reproduce the significant increasing trends in July at Alert and October at Zeppelin due to some existent model bias of Arctic cryospheric processes. The mobilization of Hg while thawing permafrost in some watersheds [*Rydberg et al.*, 2010] that contributes to riverine Hg in summer still remains unknown, including its magnitude and historical trends. Preliminary data are used to estimate the magnitude of snow/ice Hg reservoir (see section 3.2) but with large uncertainties [*St. Louis et al.*, 2007; *Beattie et al.*, 2014]. These uncertainties would contribute to the discrepancies in summer and fall.

Figure 3 maps the spatial distribution of the simulated trends of TGM north of 30°N for different seasons. The 12 months are grouped into four seasons based on the feature of seasonal variability in trends at the Arctic sites. The simulated increase in Asia reflects increasing regional anthropogenic emissions. The decrease over the North Atlantic is driven by the decreasing oceanic evasion. The simulation shows an obvious difference in trends between the Arctic and northern midlatitudes, particularly in spring and fall, with positive trends along the coast and center of the Arctic Ocean in April–May and August–October, respectively, consistent with observations.

3.2. Climatological Variables Driving the Unique Trends in the Arctic

Figure 4 shows the contributions from different environmental variables to the atmospheric Hg trends at the two Arctic sites. The atmospheric Hg decline signal at northern midlatitudes propagates to the Arctic.

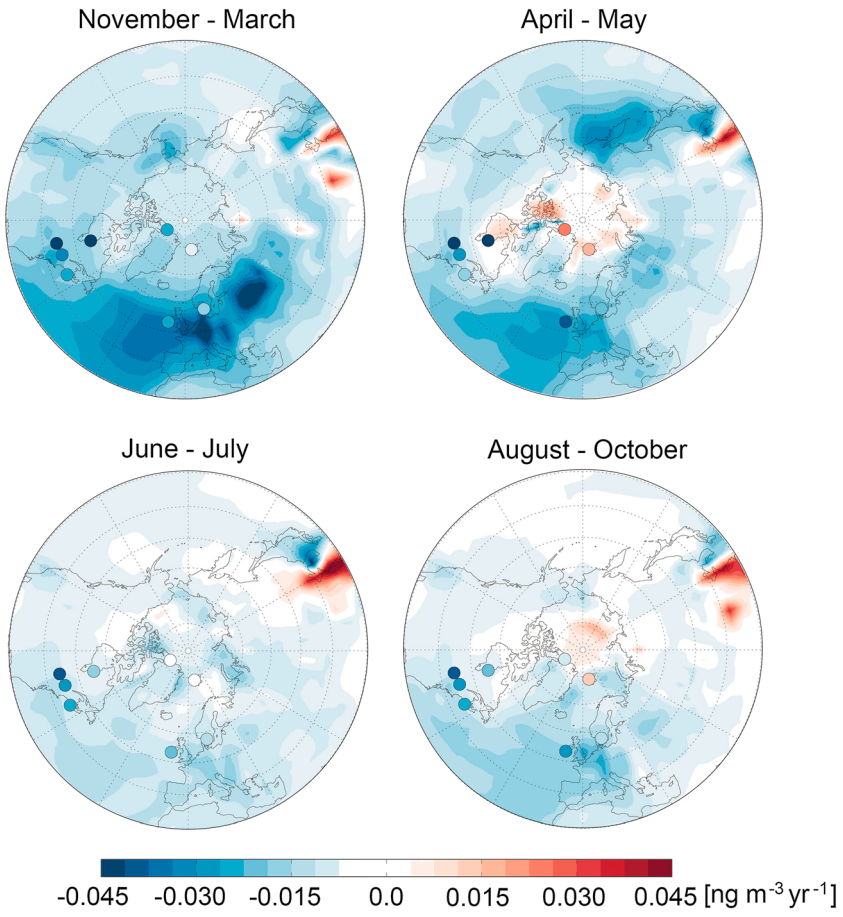

Figure 3. Trends in total gaseous mercury (TGM) north of 30°N for different seasons over the period 2000–2009. Contours show GEOS-Chem simulated values and circles show observations.

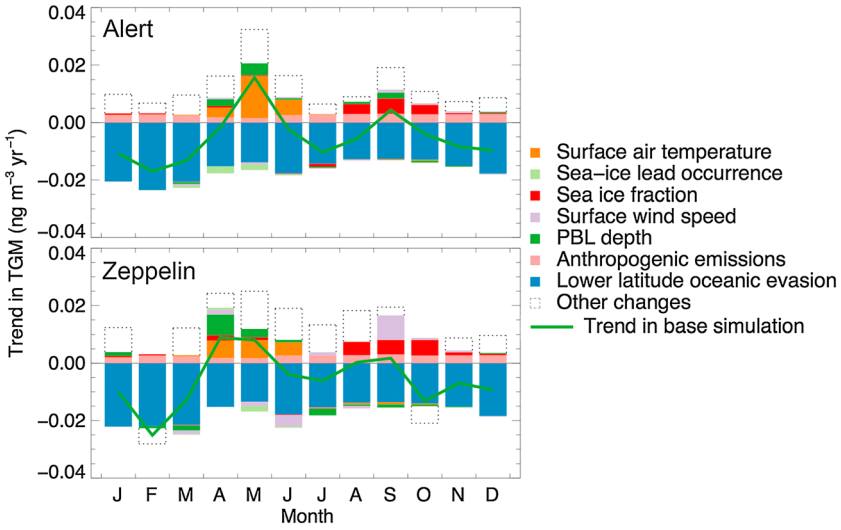

Figure 4. Trends of atmospheric Hg concentrations contributed by different environmental variables at the Arctic sites. The dashed line boxes represent contributions from other insignificant variables, changes of meteorology outside the Arctic, and interactions among variables.

Table 2. Influence of Climatological Variables With Significant Contributions on Hg Cycle in Spring and Fall Over the Arctic Ocean[a]

			Decadal Trends of Processes Related to Hg Cycle (% yr^{-1})				
Seasons	Influencing Variables	Decadal Trends of Variables (% yr^{-1})	Frequency of AMDEs	Total Hg Deposition	Oceanic Evasion	Surface air TGM Concentrations	Surface ocean Hg Concentrations
April–May	Surface air temperature	+0.08	−3.15	−1.36		+0.43	−0.08
April–May	Sea ice lead occurrence	+0.84	+2.24	+0.61		−0.19	*+0.02*[b]
August–October	Sea ice fraction (barrier)[c]	−2.49			+1.80	*+0.44*	−0.81
	Sea ice fraction (reservoir)	−0.60[d]			*+0.21*	*+0.04*	+0.20
							Total: −0.67

[a]Trends are calculated based on the average data over the Arctic Ocean.
[b]Significant trends are indicated in normal fonts ($p < 0.1$), while insignificant trends are indicated in italics.
[c]Two roles for sea ice influence on Hg cycle in August–October, including as a barrier for air-sea exchange and as a reservoir of Hg.
[d]The accelerated shrinking amount is simulated by the model which is based on the declining sea ice fraction and reservoir amount of 50 Mg we estimated.

Decreasing oceanic evasion from lower latitudes causes consistently declining trends (average −0.017 ng m^{-3} yr^{-1}), especially in November–March. Changes to global anthropogenic emissions on the other hand show consistently positive contributions (average +0.003 ng m^{-3} yr^{-1}). The different Arctic Hg trends are largely caused by climatological variables including surface air temperature, sea ice fraction, sea ice lead occurrence, PBL depth, and surface wind speed. The increasing trends observed in April–May and August–October are mainly associated with increasing surface air temperature and declining sea ice fraction, respectively. The trends would be negative throughout the year, which is consistent with northern midlatitudes, if the contributions from climatological variables were absent.

For April–May, increasing surface air temperature suppresses Hg deposition through decreasing the frequency of AMDEs and subsequently promotes the increase of atmospheric Hg, while increasing sea ice lead occurrence plays the opposite role. These two variables largely determine the frequency of AMDEs. We simulate the frequency of AMDEs of 34.9% and 22.0% at Alert and Zeppelin, respectively, consistent with observations (35.6% and 14.9%, respectively). The increasing surface air temperature (+0.08% yr^{-1}) results in the decreasing frequency of AMDEs (−3.15% yr^{-1}), which causes a −1.36% yr^{-1} (−0.72 Mg yr^{-1}) decrease of total Hg deposition over the Arctic Ocean and a subsequent +0.43% yr^{-1} increase of surface air TGM concentrations (Table 2). Conversely, the increasing sea ice lead occurrence (+0.84% yr^{-1}) increases the frequency of AMDEs (+2.24% yr^{-1}), which causes a +0.61% yr^{-1} (+0.32 Mg yr^{-1}) increase of total Hg deposition and a subsequent −0.19% yr^{-1} decrease of surface air TGM concentrations.

For August–October, declining sea ice fraction decreases the barrier for air-sea exchange [*Hirdman et al.*, 2009] and promotes oceanic evasion, which subsequently increases atmospheric Hg. *Fisher et al.* [2013] suggested this effect in June–July during 1979–2008. Due to the weak trend of sea ice fraction in these 2 months over the period 2000–2009 (Table 1), the contribution from sea ice fraction to oceanic evasion and atmospheric Hg is not found for June–July in this study. Instead, we find this effect in August–October, where the declining sea ice fraction (−2.49% yr^{-1}) results in increasing oceanic evasion (+1.80% yr^{-1}; +0.65 Mg yr^{-1}) and subsequently increasing surface air TGM concentrations (+0.44% yr^{-1}; not significant) (Table 2). In addition, the melting of multiyear sea ice and snow releases Hg to ocean water that is readily reducible and available for evasion [*Fisher et al.*, 2012]. Based on the observed Hg concentrations in multiyear sea ice (average 7.4 pM [*Beattie et al.*, 2014]) and Hg loads on snow over sea ice (5.18 mg ha^{-1} [*St. Louis et al.*, 2007]), we estimate approximately 50 Mg of Hg in this reservoir. The accelerated shrinking of this reservoir (−0.60% yr^{-1}; −0.3 Mg yr^{-1}) contributes little to atmospheric Hg trends due to its small contribution to trends in oceanic evasion (+0.21% yr^{-1}; +0.08 Mg yr^{-1}; not significant) (Table 2).

The signs of contributions from PBL depth and surface wind speed vary in different months (Figure 4), resulting from the variation of decadal trends of these variables in different seasons (Table 1). *Fisher et al.* [2013] found increasing wind speed in spring and early summer resulted in enhanced atmospheric turbulence over large sea ice coverage, which promoted deposition and caused a decline of surface air Hg concentrations. However, we find that this effect is offset by the increasing oceanic evasion in fall when sea ice coverage is small. The increasing wind speed results in larger piston velocity and ultimately increases surface air Hg concentrations in fall.

4. Implications and Summary

The weaker and more variable trends of atmospheric Hg in the Arctic relative to northern midlatitudes reflect a combination of decreasing Hg deposition ($-0.40\,\mathrm{Mg\,yr^{-1}}$) in spring and increasing oceanic evasion ($+0.73\,\mathrm{Mg\,yr^{-1}}$) in fall driven by climatological variables (specifically surface air temperature and sea ice fraction). This implies a decline of Hg in the Arctic surface ocean that we estimate to be $-0.67\%\,\mathrm{yr^{-1}}$ over the period 2000–2009 (Table 2).

Future forcing scenarios [*Intergovernmental Panel on Climate Change*, 2007, 2013] suggest that some climate warming signals, such as high surface air temperatures, low sea ice extent, and strong warming in spring will intensify in future decades. This would drive a sustained increase in Arctic atmospheric Hg and decline in Arctic Ocean Hg, as the ocean is expected to remain supersaturated relative to the atmosphere in future decades [*Andersson et al*., 2008]. This "turbulence" caused by climatological variables will result in synergistic effects with Hg policies on the Arctic Hg pollution. Policies on climate warming controls may slow down the decline in surface ocean Hg, which calls for stricter policies on Hg emission controls. Bilateral cooperation will be strengthened between Hg and climate change groups to address the pollution.

Changing climatological variables could affect processes such as methylation, demethylation, and bioaccumulation [*Point et al*., 2011; *Braune et al*., 2015]. The decline in surface ocean Hg could not necessarily imply a reduction of Hg in Arctic biota, as suggested by the increasing trends found in Arctic marine mammals from previous studies [*Riget et al*., 2011]. More detailed studies with Hg methylation and its trophic transfer in the Arctic are thus needed. The Arctic Hg budget is still under debate in literatures [*Dastoor and Durnford*, 2013], as summarized by *AMAP* [2011], which suggested differences in simulated flux from different models. However, the effects of increasing air temperature and decreasing sea ice extent on the Arctic Hg cycle are consistent. Alternative hypothesis have also been proposed [*Slemr et al*., 2011; *Horowitz et al*., 2014] for the decline of atmospheric Hg in northern midlatitudes. Although the exact reason driving this trend is beyond the scope of this study, their effects on the Arctic Hg trends are similar.

Overall, this study suggests that climatological variables drive the unique atmospheric Hg trends in the Arctic relative to northern midlatitudes. The driving processes suggest that Arctic Ocean Hg is declining and is expected to continue to decline due to rapid Arctic warming and declining sea ice in future decades.

Acknowledgments
We acknowledge financial support for this work from the U.S. National Science Foundation and China Scholarship Council (201306010173). Xuejun Wang acknowledges support from the National Natural Science Foundation of China (41130535). We thank Elsie M. Sunderland and Helen M. Amos for their helpful discussions. All data for this paper are properly cited and referred to in the reference list.

The Editor thanks two anonymous reviewers for their assistance in evaluating this paper.

References

Arctic Monitoring and Assessment Programme (AMAP) (2011), *AMAP Assessment 2011: Mercury in the Arctic*, pp. 26–36, 159–170, Oslo, Norway, Arctic Monitoring and Assessment Programme.

AMAP/United Nations Environment Programme (2013), *Technical Background Report for the Global Mercury Assessment 2013*, pp. 4–37, Arctic Monitoring and Assessment Programme, Oslo, Norway/UNEP Chemicals Branch, Geneva, Switzerland.

Amos, H. M., D. J. Jacob, D. G. Streets, and E. M. Sunderland (2013), Legacy impacts of all-time anthropogenic emissions on the global mercury cycle, *Global Biogeochem. Cycles*, *27*, 410–421, doi:10.1002/gbc.20040.

Amos, H. M., D. J. Jacob, D. Kocman, H. M. Horowitz, Y. Zhang, S. Dutkiewicz, M. Horvat, E. S. Corbitt, D. P. Krabbenhoft, and E. M. Sunderland (2014), Global biogeochemical implications of mercury discharges from rivers and sediment burial, *Environ. Sci. Technol.*, *48*(16), 9514–9522, doi:10.1021/es502134t.

Andersson, M. E., J. Sommar, K. Gårdfeldt, and O. Lindqvist (2008), Enhanced concentrations of dissolved gaseous mercury in the surface waters of the Arctic Ocean, *Mar. Chem.*, *110*(3–4), 190–194, doi:10.1016/j.marchem.2008.04.002.

Arrigo, K. R., and G. L. van Dijken (2011), Secular trends in Arctic Ocean net primary production, *J. Geophys. Res.*, *116*, C09011, doi:10.1029/2011JC007151.

Beattie, S. A., D. Armstrong, A. Chaulk, J. Comte, M. Gosselin, and F. Wang (2014), Total and methylated mercury in Arctic multiyear sea ice, *Environ. Sci. Technol.*, *48*(10), 5575–5582, doi:10.1021/es5008033.

Bekryaev, R. V., I. V. Polyakov, and V. A. Alexeev (2010), Role of polar amplification in long-term surface air temperature variations and modern Arctic warming, *J. Clim.*, *23*(14), 3888–3906, doi:10.1175/2010JCLI3297.1.

Berg, T., K. A. Pfaffhuber, A. S. Cole, O. Engelsen, and A. Steffen (2013), Ten-year trends in atmospheric mercury concentrations, meteorological effects and climate variables at Zeppelin, Ny-Ålesund, *Atmos. Chem. Phys.*, *13*(13), 6575–6586, doi:10.5194/acp-13-6575-2013.

Braune, B., et al. (2015), Mercury in the marine environment of the Canadian Arctic: Review of recent findings, *Sci. Total Environ.*, *509–510*, 67–90, doi:10.1016/j.scitotenv.2014.05.133.

Cobbett, F. D., A. Steffen, G. Lawson, and B. J. Van Heyst (2007), GEM fluxes and atmospheric mercury concentrations (GEM, RGM and Hg^P) in the Canadian Arctic at Alert, Nunavut, Canada (February–June 2005), *Atmos. Environ.*, *41*(31), 6527–6543, doi:10.1016/j.atmosenv.2007.04.033.

Cole, A. S., and A. Steffen (2010), Trends in long-term gaseous mercury observations in the Arctic and effects of temperature and other atmospheric conditions, *Atmos. Chem. Phys.*, *10*(10), 4661–4672, doi:10.5194/acp-10-4661-2010.

Cole, A. S., A. Steffen, K. A. Pfaffhuber, T. Berg, M. Pilote, L. Poissant, R. Tordon, and H. Hung (2013), Ten-year trends of atmospheric mercury in the high Arctic compared to Canadian sub-Arctic and mid-latitude sites, *Atmos. Chem. Phys.*, *13*(3), 1535–1545, doi:10.5194/acp-13-1535-2013.

Corbitt, E. S., D. J. Jacob, C. D. Holmes, D. G. Streets, and E. M. Sunderland (2011), Global source-receptor relationships for mercury deposition under present-day and 2050 emissions scenarios, *Environ. Sci. Technol.*, *45*(24), 10,477–10,484, doi:10.1021/es202496y.

Dastoor, A. P., and D. A. Durnford (2013), Arctic Ocean: Is it a sink or a source of atmospheric mercury?, *Environ. Sci. Technol.*, *48*(3), 1707–1717, doi:10.1021/es404473e.

Ebinghaus, R., S. G. Jennings, H. H. Kock, R. G. Derwent, A. J. Manning, and T. G. Spain (2011), Decreasing trends in total gaseous mercury observations in baseline air at Mace Head, Ireland from 1996 to 2009, *Atmos. Environ.*, *45*(20), 3475–3480, doi:10.1016/j.atmosenv.2011.01.033.

Fisher, J. A., D. J. Jacob, A. L. Soerensen, H. M. Amos, A. Steffen, and E. M. Sunderland (2012), Riverine source of Arctic Ocean mercury inferred from atmospheric observations, *Nat. Geosci.*, *5*(7), 499–504, doi:10.1038/NGEO1478.

Fisher, J. A., D. J. Jacob, A. L. Soerensen, H. M. Amos, E. S. Corbitt, D. G. Streets, Q. Wang, R. M. Yantosca, and E. M. Sunderland (2013), Factors driving mercury variability in the Arctic atmosphere and ocean over the past 30 years, *Global Biogeochem. Cycles*, *27*, 1226–1235, doi:10.1002/2013GB004689.

Gilbert, R. O. (1987), *Statistical Methods for Environmental Pollution Monitoring*, pp. 204–240, Van Nostrand Reinhold Company, New York.

Gustin, M., and D. Jaffe (2010), Reducing the uncertainty in measurement and understanding of mercury in the atmosphere, *Environ. Sci. Technol.*, *44*(7), 2222–2227, doi:10.1021/es902736k.

Hirdman, D., K. Aspmo, J. F. Burkhart, S. Eckhardt, H. Sodemann, and A. Stohl (2009), Transport of mercury in the Arctic atmosphere: Evidence for a spring-time net sink and summer-time source, *Geophys. Res. Lett.*, *36*, L12814, doi:10.1029/2009GL038345.

Holmes, C. D., D. J. Jacob, E. S. Corbitt, J. Mao, X. Yang, R. Talbot, and F. Slemr (2010), Global atmospheric model for mercury including oxidation by bromine atoms, *Atmos. Chem. Phys.*, *10*(24), 12,037–12,057, doi:10.5194/acp-10-12037-2010.

Horowitz, H. M., D. J. Jacob, H. M. Amos, D. G. Streets, and E. M. Sunderland (2014), Historical mercury releases from commercial products: Global environmental implications, *Environ. Sci. Technol.*, *48*(17), 10,242–10,250, doi:10.1021/es501337j.

Intergovernmental Panel on Climate Change (2007), *Climate Change 2007: The Physical Science Basis. Contribution of Working Group I to the Fourth Assessment Report of the Intergovernmental Panel on Climate Change*, edited by S. Solomon et al., Cambridge Univ. Press, Cambridge, U. K., and New York.

Intergovernmental Panel on Climate Change (IPCC) (2013), *Climate Change 2013: The Physical Science Basis. Contribution of Working Group I to the Fifth Assessment Report of the Intergovernmental Panel on Climate Change*, edited by T. F. Stocker et al., Cambridge Univ. Press, Cambridge, U. K., and New York.

Laurier, F. J. G., R. P. Mason, G. A. Gill, and L. Whalin (2004), Mercury distributions in the North Pacific Ocean—20 years of observations, *Mar. Chem.*, *90*(1–4), 3–19, doi:10.1016/j.marchem.2004.02.025.

Lindberg, S., R. Bullock, R. Ebinghaus, D. Engstrom, X. Feng, W. Fitzgerald, N. Pirrone, E. Prestbo, and C. Seigneur (2007), A synthesis of progress and uncertainties in attributing the sources of mercury in deposition, *Ambio*, *36*(1), 19–33, doi:10.1579/0044-7447(2007)36[19:ASOPAU]2.0.CO;2.

Mason, R. P., N. M. Lawson, and G. R. Sheu (2001), Mercury in the Atlantic Ocean: Factors controlling air-sea exchange of mercury and its distribution in the upper waters, *Deep Sea Res., Part II*, *48*(13), 2829–2853, doi:10.1016/S0967-0645(01)00020-0.

Mergler, D., H. A. Anderson, L. H. M. Chan, K. R. Mahaffey, M. Murray, M. Sakamoto, and A. H. Stern (2007), Methylmercury exposure and health effects in humans: A worldwide concern, *Ambio*, *36*(1), 3–11, doi:10.1579/0044-7447(2007)36[3:MEAHEI]2.0.CO;2.

Parkinson, C. L., and D. J. Cavalieri (2008), Arctic sea ice variability and trends, 1979–2006, *J. Geophys. Res.*, *113*, C07003, doi:10.1029/2007JC004558.

Pöhler, D., L. Vogel, U. Frieß, and U. Platt (2010), Observation of halogen species in the Amundsen Gulf, Arctic, by active long-path differential optical absorption spectroscopy, *Proc. Natl. Acad. Sci. U.S.A.*, *107*(15), 6582–6587, doi:10.1073/pnas.0912231107.

Point, D., J. E. Sonke, R. D. Day, D. G. Roseneau, K. A. Hobson, S. S. Vander Pol, A. J. Moors, R. S. Pugh, O. F. X. Donard, and P. R. Becker (2011), Methylmercury photodegradation influenced by sea-ice cover in Arctic marine ecosystems, *Nat. Geosci.*, *4*(3), 188–194, doi:10.1038/ngeo1049.

Rienecker, M. M., et al. (2011), MERRA: NASA's Modern-Era Retrospective Analysis for Research and Applications, *J. Clim.*, *24*(14), 3624–3648, doi:10.1175/JCLI-D-11-00015.1.

Riget, F., et al. (2011), Temporal trends of Hg in Arctic biota, an update, *Sci. Total Environ.*, *409*(18), 3520–3526, doi:10.1016/j.scitotenv.2011.05.002.

Rydberg, J., J. Klaminder, P. Rosén, and R. Bindler (2010), Climate driven release of carbon and mercury from permafrost mires increases mercury loading to sub-Arctic lakes, *Sci. Total Environ.*, *408*(20), 4778–4783, doi:10.1016/j.scitotenv.2010.06.056.

St. Louis, V. L., H. Hintelmann, J. A. Graydon, J. L. Kirk, J. Barker, B. Dimock, M. J. Sharp, and I. Lehnherr (2007), Methylated mercury species in Canadian high Arctic marine surface waters and snowpacks, *Environ. Sci. Technol.*, *41*(18), 6433–6441, doi:10.1021/es070692s.

Shiklomanov, A. I., and R. B. Lammers (2009), Record Russian river discharge in 2007 and the limits of analysis, *Environ. Res. Lett.*, *4*(4), 045015, doi:10.1088/1748-9326/4/4/045015.

Slemr, F., E. G. Brunke, R. Ebinghaus, and J. Kuss (2011), Worldwide trend of atmospheric mercury since 1995, *Atmos. Chem. Phys.*, *11*(10), 4779–4787, doi:10.5194/acp-11-4779-2011.

Soerensen, A. L., E. M. Sunderland, C. D. Holmes, D. J. Jacob, R. M. Yantosca, H. Skov, J. H. Christensen, S. A. Strode, and R. P. Mason (2010), An improved global model for air-sea exchange of mercury: High concentrations over the North Atlantic, *Environ. Sci. Technol.*, *44*(22), 8574–8580, doi:10.1021/es102032g.

Soerensen, A. L., D. J. Jacob, D. G. Streets, M. L. I. Witt, R. Ebinghaus, R. P. Mason, M. Andersson, and E. M. Sunderland (2012), Multi-decadal decline of mercury in the North Atlantic atmosphere explained by changing subsurface seawater concentrations, *Geophys. Res. Lett.*, *39*, L21810, doi:10.1029/2012GL053736.

Streets, D. G., M. K. Devane, Z. F. Lu, T. C. Bond, E. M. Sunderland, and D. J. Jacob (2011), All-time releases of mercury to the atmosphere from human activities, *Environ. Sci. Technol.*, *45*(24), 10,485–10,491, doi:10.1021/es202765m.

Wilson, S., J. Munthe, K. Sundseth, K. Kindbom, P. Maxson, J. Pacyna, and F. Steenhuisen (2010), Updating historical global inventories of anthropogenic mercury emissions to air, AMAP Tech. Rep. 3, pp. 1–12, Arctic Monitoring and Assessment Programme, Oslo, Norway.